INDSWG-132

IDO-17134
EANDC(US)-84 "U"
INDC(US)-2 "U"
January 1966

COMPILATION OF RESOLUTIONS AND INTENSITIES OF SLOW NEUTRON, INELASTIC SCATTERING, TIME-OF-FLIGHT INSTRUMENTS

R. M. Brugger and Y. D. Harker

PHILLIPS PETROLEUM COMPANY

PHILLIPS 66

ATOMIC ENERGY DIVISION

NATIONAL REACTOR TESTING STATION
US ATOMIC ENERGY COMMISSION

PRINTED IN USA. PRICE $2.00. AVAILABLE FROM THE CLEARINGHOUSE FOR FEDERAL SCIENTIFIC AND TECHNICAL INFORMATION, NATIONAL BUREAU OF STANDARDS U. S. DEPARTMENT OF COMMERCE, SPRINGFIELD, VIRGINIA

IDO-17134
EANDC(US)-84 "U"
INDC(US)-2 "U"
AEC Research and Development Report
Instruments
TID-4500 (47th Ed.)
Issued: January 1966

COMPILATION OF RESOLUTIONS AND INTENSITIES OF SLOW NEUTRON, INELASTIC SCATTERING, TIME-OF-FLIGHT INSTRUMENTS

BY

R. M. Brugger

Y. D. Harker

PHILLIPS
PETROLEUM
COMPANY

Atomic Energy Division
Contract AT(10-1)-205
Idaho Operations Office
U. S. ATOMIC ENERGY COMMISSION

CONTENTS

TABLES

FIGURES

COMPILATION OF RESOLUTIONS AND INTENSITIES OF SLOW NEUTRON, INELASTIC SCATTERING, TIME-OF-FLIGHT INSTRUMENTS

I. INTRODUCTION

This compilation is an attempt to present intensities and resolutions of all slow neutron, inelastic scattering instruments that use time-of-flight methods. The theory of resolution of phased choppers as presented by Royston[1] is the basis for the analysis. However, since full widths at half maximum of bursts are more widely used than standard deviations, Royston's equations have been converted from standard deviations to half widths. The authors know that this is not exact, but they felt that it was necessary to encourage a response from other scientists. So long as the shapes of the time-of-flight and time distributions can be approximated by a triangle, this change does not introduce large errors.

Using the defininitions of this compilation, the scientists actually using the instruments were asked to supply their intensities and resolution. In some cases these definitions do not exactly fit a scientist's instrument; or his interpretation of the resolutions and intensities has been somewhat different from those of the authors. In the tables the difference[a] in interpretations by the scientists is indicated wherever it occurs. The equations of Royston that are used are for a phased chopper system in which both choppers have equal burst times. Thus, for rotating crystal spectrometers, filter choppers, and linear accelerators plus choppers, the equations are only approximations.

To determine resolution, Equation (1) was obtained by the following arguments. Start with Royston's Equation (7)

$$\sigma_{tR}^{2}(X_R) = X_R^{2}\,\sigma_{\tau R}^{2} + \sigma_{tR}^{2}(0)$$

(where the subscript R refers to parameters as defined by Royston and no subscript refers to the definitions in this compilation). To convert Royston's Equation (7) to the notation of this compilation the following conversions were used:

(a) $x + d = X_R$

---

[a] In the requests to the scientists for information, Equations (1) and (2) were misstated as

$$\Delta t_o^{\,2} = \Delta\tau^2 + (x+d)^2\left(\frac{\Delta E_o}{E_o}\right)^2\left(\frac{1.3 \times 10^3}{E_o}\right).$$

and

$$\Delta t_f^{\,2} = \Delta\tau^2 + \left[x + \left(\frac{E_o}{E_f}\right)^{3/2} d\right]^2 \left(\frac{\Delta E_o}{E_o}\right)^2\left(\frac{1.3 \times 10^3}{E_o}\right).$$

Corrections have been made for this error so that the tables are consistent with Equations (1) and (2).

(b) $2\Delta t = \Delta t_R$

Using Royston's Equation (22) where $\sigma_{tR}(0) = \frac{\Delta t_R}{4\sqrt{3}}$ one gets

(c) $\frac{\Delta\tau}{2\sqrt{3}} = \sigma_{tR}(0)$

(d_1) For any triangular distribution (0.8) (full width at half maximum) ≈ 2(standard deviation)

(d_2) For the energy distribution in particular, full width at half maximum for time of flight/time of flight = $(1/2)\ (\Delta E/E)$

(d_3) Time of flight (μsec/m) = $\frac{72.3}{\sqrt{E_o(\text{eV})}}$.

In combining d_1, d_2, and d_3 one gets

$$2\sigma_{\tau R} = (0.8)\ (1/2)\ \left(\frac{\Delta E}{E}\right) \frac{72.3}{\sqrt{E_o}}$$

and finally

(d_4)
$$2\sigma_{\tau R} = (0.8)\ \left(\frac{\Delta E}{E}\right) \sqrt{\frac{1310}{E}}$$

Substituting in Royston's Equation (7) the relations found in a, b, c, and d_4, one obtains

$$(0.4)^2\ \Delta t^2 = (x + d)^2\ (0.4)^2\ \left(\frac{\Delta E_o}{E_o}\right)^2 \left(\frac{1310}{E_o}\right) + \frac{\Delta\tau}{(4)(3)}$$

which reduces to

$$\Delta t^2 = (x + d)^2 \left(\frac{\Delta E_o}{E_o}\right)^2 \left(\frac{1310}{E_o}\right) + \frac{\Delta\tau^2}{1.92}$$

which approximates

$$\Delta t_o^{\ 2} \approx \frac{1}{2}\ \Delta^2 + (x + d)^2 \left(\frac{\Delta E_o}{E_o}\right)^2 \left(\frac{1.3 \times 10^3}{E_o}\right) .$$

Equation (2) can be obtained in a similar manner from Equation (47) of Royston.

In Tables I through XXIII, intensities and resolutions are given for each instrument at a set of incident energies that cover their normal range of operation. Whenever possible, measured values are used. The "Resolution (elastic)" represents the resolution for elastic scattering, while "Resolution (inelastic)" is an attempt to show the resolution when neutrons are inelastically scattered by the sample. In the latter case, 0.025 eV was arbitrarily selected as the mean final neutron energy in all cases. In this case $\Delta t_f/t_f$ represents the error in timing the burst of neutrons that are inelastically scattered while $\Delta\epsilon/\epsilon$ was selected to represent the error in measuring the change in energy

when both the incident energy and the final energy must be determined by time of flight and when these measurements are uncorrelated.

The intensities and resolutions for each instrument are given in a separate table, and a standard format is used to aid in comparing one instrument to another. Figures 1 through 9 are an attempt to present data for several instruments in one display. The attempt is only partially successful since the graphs cannot show the dependence of intensity on such parameters as angular resolution; they show but do not compensate for different incident energies.

II. EQUATIONS

(1) $$\Delta t_o^{\,2} = \frac{1}{2}\Delta\tau^2 + (x + d)^2 \left(\frac{\Delta E_o}{E_o}\right)^2 \left(\frac{1.31 \times 10^3}{E_o}\right)$$

(2) $$\Delta t_f^{\,2} = \frac{1}{2}\Delta\tau^2 + \left[x + \left(\frac{E_o}{E_f}\right)^{3/2} d\right]^2 \left(\frac{\Delta E_o}{E_o}\right)^2 \left(\frac{1.31 \times 10^3}{E_o}\right)$$

(3) $$\Delta\epsilon^2 = 4\left[E_f^{\,2}\left(\frac{\Delta t_f}{t_f}\right)^2 + E_o^{\,2}\left(\frac{\Delta t_o}{t_o}\right)^2\right]$$

III. DEFINITIONS

Flight Path: The distance d in meters from the sample to the detectors.

Source Flux: The thermal neutron flux/cm^2sec at the bottom of the beam hole.

I(n/cm^2min): The intensity of monoenergetic thermal neutrons/cm^2min at the sample position.

I(n/min): The intensity of monoenergetic thermal neutrons/min over the complete beam area at the sample position.

Resolution: The energy, time resolution, and combined energy-time resolution for scattering neutrons.

E_o: The mean energy in eV of the incident monoenergetic beam.

ΔE_o: The full width at half maximum of the energy spread in eV in the monoenergetic beam.

$\Delta\tau$: The full width at half maximum in μsec of only the time spread in the monoenergetic beam. (In the MTR Velocity Selector this is the full width at half maximum of the burst when measured right after the last chopper.)

t_o: The time of flight in μsec of the elastically scattered neutrons to travel from the sample to the detector.

Δt_o: The full width at half maximum in μsec of the burst of elastically scattered neutrons as measured in time at the detectors.

E_f: The mean energy in eV of the neutrons inelastically scattered with a discrete energy change.

t_f: The time of flight in μsec of the inelastically scattered neutrons to travel from the sample to the detectors.

Δt_f: The full width at half maximum in μsec of the burst of inelastically scattered neutrons as measured in time at the detectors.

x: The distance in meters from the "effective chopping point" (see Royston) to the sample position. (For a system consisting of two identical choppers rotating at the same speed, the effective chopping point is midway between choppers.)

ϵ: The discrete energy change in eV of the neutrons involved in an inelastic scattering process when the final mean energy of the neutrons in 0.025 eV.

$\Delta\epsilon$: The uncertainty in measuring ϵ in eV due to the finite widths

in time of the incident and scattered bursts for the inelastic case. $\Delta\epsilon$ is computed using Equation (3).

Signal/background: The ratio of the total number of counts in the time interval spanned by the vanadium elastic scattering peak to the background counts in the same interval.

Sample Thickness: The thickness parallel to the incident beam in centimeters of the vanadium sample.

Scattering Angle: Angle of scattering relative to the incident beam in degrees at which the signal/background was measured.

Range: The normal range of the scattering angles of the instrument.

No. of Detector Banks: Number of detector banks at different scattering angles used simultaneously.

Solid Angle per Detector Bank: The solid angle subtended by each detector bank.

Kind of Detector: The kind of detector normally used in the detector banks (ie, 1 in. x 18 in. 167-cm BF_3 detector or 5 in. diameter Li loaded glass scintillation detector, etc.).

IV. REFERENCE

1. R. J. Royston, "The Resolution Function of a Two-Rotor Neutron Velocity Selector", Nuclear Instruments and Methods, 30 (1964) pp 184-202.

TABLE I

COLD NEUTRON CHOPPER -- HARWELL

Instrument: Cold Neutron Chopper

Location: DIDO Reactor, Atomic Energy Research Establishment, Harwell

Reference: Harris, Cocking, Egelstaff, and Webb, Proceedings of the Chalk River Conference on "Inelastic Scattering of Neutrons in Solids and Liquids", Vol. 1, p 107, I.A.E.A., Vienna (1963).

Beam Size: 5.08 cm x 2.54 cm

Flight Path: 1.3 m

Source Flux: 5×10^{13} thermal neutrons/cm^2-sec (liquid H_2 source increases this by X4 at 0.005 eV)

Intensity Determination: Measured

Intensity:

E_o(eV)	I(n/min)	I(n/cm^2-min)
0.005 eV (37,500 rpm[a])	2.0×10^6[b]	1.6×10^5[b]
0.005 eV (28,300 rpm[a])	2.4×10^6[b]	1.9×10^5[b]
0.005 eV (18,700 rpm[a])	4.4×10^6[b]	3.4×10^5[b]

Resolution (elastic):

	Energy Distribution of Burst		Time Distribution of Burst		Burst Width at Detector	
E_o(eV)	ΔE_o(eV)	$\Delta E_o/E_o$	$\Delta\tau$(μsec)	$\Delta\tau/t_o$	Δt_o(μsec)	$\Delta t_o/t_o$
0.005 eV (28,300 rpm[a])	0.0005	0.10	16	0.012	100	0.074

Resolution (inelastic):

		Burst Width at Detector			Uncertainty in Energy Change	
E_o(eV)	E_f(eV)	Δt_f(μsec)	t_f/t_f	ε(eV)	$\Delta\varepsilon$(eV)	$\Delta\varepsilon/\varepsilon$
0.005 eV (28,300 rpm[a])	0.025	44[c]	0.073	0.020	0.0037[d]	0.19

[a] Angular velocity of chopper.

[b] Intensities recorded are with liquid hydrogen source.

[c] Computed from Equation (2) with x = 0.64 computed from Equation (1).

[d] Computed from Equation (3).

TABLE II

COLD NEUTRON CHOPPER -- BIRMINGHAM UNIVERSITY

Instrument: Cold Neutron Chopper

Location: HERALD Reactor, A.W.R.E., Aldermaston

Reference: Ph.D. Thesis, F. P. Szabo, 1965.

Beam Size: 4.5 cm x 2.5 cm at the rotor axis (also at sample position)

Flight Path: 1.6 meters

Source Flux: 2×10^{12} thermal neutrons/cm^2-sec. The experiment makes use of a 15 cm tangential beam tube. The quoted flux is that measured at the source position, with the tube filled with water.

Intensity Determination:

Intensity:

E_0(eV)	I(n/min)	I(n/cm^2-min)
0.005	2.2×10^5	1.94×10^4

NOTE: These intensities will be considerably increased when a cold source is installed toward the end of 1965.

Resolution (elastic):

	Energy Distribution of Burst		Time Distribution of Burst		Burst Width at Detector	
E_0(eV)	ΔE_0(eV)	$\Delta E_0/E_0$	$\Delta\tau$(μsec)	$\Delta\tau/t_0$	Δt_0(μsec)	$\Delta t_0/t_0$
0.005	0.00125	0.25	11.5	0.0072	242	0.15

Resolution (inelastic):

		Burst Width at Detector			Uncertainty in Energy Change	
E_0(eV)	E_f(eV)	Δt_f(μsec)	$\Delta t_f/t_f$	ε(eV)	$\Delta\varepsilon$(eV)	$\Delta\varepsilon/\varepsilon$
0.005	0.025	57[a]	0.078	0.02	0.0042	0.21

Signal/Background:

E_0(eV)	V Sample Thickness (cm)	Scattering Angle (degrees)	Signal/Background
0.005	0.28	50	40

Scattering Angles:

Range (degrees)	Number of Detector Banks	Flight Path (m)	Solid Angle per Detector Bank (steradian)	Kind of Detector
20 to 90	8	1.6	0.0078	Proportional Counter Enriched BF_3 5 cm diameter 40 cm active length 70 cm pressure

[a] Computed from Equation (2) with x = 0.3 calculated from Equation (1).

TABLE III

COLD NEUTRON CHOPPER -- BROOKHAVEN NATIONAL LABORATORY

Instrument: Cold Neutron Chopper

Location: HFBR, Brookhaven National Laboratory

Reference: K. Otnes and H. Palevsky, Proceedings of the Chalk River Conference on "Inelastic Scattering of Neutrons in Solids and Liquids", Vol. 1, p 95, I.A.E.A., Vienna (1963).

Beam Size: 1.25 cm x 5 cm

Flight Path: 1.6 m

Source Flux: 5×10^{14} thermal neutrons/cm^2-sec

Intensity Determination: Calculated

Intensity:

E_o(eV)	I(n/min)	I(n/cm^2-min)
0.005 (one rotor system)	4.8×10^8	7.7×10^7
0.005 (two rotor system)	2.4×10^8	3.8×10^7
0.005 (three rotor system)	3.0×10^7	4.8×10^6

Resolution (elastic):

	Energy Distribution of Burst		Time Distribution of Burst		Burst Width at Detector	
E_o(eV)	ΔE_o(eV)	$\Delta E_o/E_o$	$\Delta\tau$(μsec)	$\Delta\tau/t_o$	Δt_o(sec)	$\Delta t_o/t_o$
0.005 (one rotor system)	0.00065	0.125	25.0	0.016	128[a]	0.08
0.005 (two rotor system)	0.00033	0.0625	12.5	0.008	64[a]	0.04
0.005 (three rotor system)	0.00016	0.0315	12.5	0.008	40[a]	0.025

Resolution (inelastic):

		Burst Width at Detector			Uncertainty in Energy Change	
E_o(eV)	E_f(eV)	Δt_f(μsec)	$\Delta t_f/t_f$	ε(eV)	$\Delta\varepsilon$(eV)	$\Delta\varepsilon/\varepsilon$
0.005 (one rotor system)	0.025	39[b]	0.053	0.02	0.0028[c]	0.14
0.005 (two rotor system)	0.025	19[b]	0.027	0.02	0.0014[c]	0.072
0.005 (three rotor system)	0.025	18[b]	0.024	0.02	0.0012[c]	0.061

[a] Assuming x = 0.4, 0.4, and 0.8 for the three cases.

[b] Assuming sample immediately after last chopper.

[c] Computed from Equation (3).

TABLE IV

COLD NEUTRON CHOPPER -- ARGONNE NATIONAL LABORATORY

Instrument: New Cold Neutron Chopper (completion November 1, 1965)

Location: CP-5 Reactor, Argonne National Laboratory

Reference: D. Connor (private communication).

Beam Size: 3 cm x 1 cm

Flight Path: 4.0 meters

Source Flux: Approximately 5×10^{12} thermal neutrons/cm^2-sec (cold source, $T_n \approx 50°K$)

Intensity Determination: Estimated (duty cycle included)

Intensity:

E_o(eV)	I(n/min)	I(n/cm^2-min)
0.00495	1.5×10^6	5.0×10^5

Resolution (elastic):

	Energy Distribution of Burst		Time Distribution of Burst		Burst Width at Detector	
E_o(eV)	ΔE_o(eV)	$\Delta E_o/E_o$	$\Delta\tau$(μsec)	$\Delta\tau/t_o$	Δt_o(μsec)	$\Delta t_o/t_o$
0.00495	0.0005	0.1	5	0.00125	212[a]	0.053

Resolution (inelastic):

		Burst Width at Detector			Uncertainty in Energy Change	
E_o(eV)	E_f(eV)	Δt_f(μsec)	$\Delta t_f/t_f$	ε(eV)	$\Delta\varepsilon$(eV)	$\Delta\varepsilon/\varepsilon$
0.00495	0.025	18.5[b]	0.01	0.020	0.0005[c]	0.025

Signal/Background:

E_o(eV)	V Sample Thickness (cm)	Scattering Angle (degrees)	Signal/Background

Scattering Angles:

Range (degrees)	Number of Detector Banks	Flight Path (m)	Solid Angle per Detector Bank (steradian)	Kind of Detector
15 to 120	81	4	0.0087	BF_3 (160 cm pressure)

[a] Calculated from Equation (1).

[b] Calculated from Equation (2).

[c] Calculated from Equation (3).

TABLE V

COLD NEUTRON CHOPPER -- PICATINNY ARSENAL

Instrument: Cold Neutron Chopper

Location: AMRA Reactor, Watertown, Massachusetts

Reference: Boutin, Prask, and Trevino (private communication).

Beam Size: 7.5 cm x 7.5 cm

Flight Path: 5.03 meters

Source Flux: 10^{12} thermal neutrons/cm^2-sec

Intensity Determination: Measured

Intensity:

E_0(eV)	I(n/min)	I(n/cm^2-min)
0.005	1.5×10^{9} [a]	2.4×10^{7} [a]

Resolution (elastic):

	Energy Distribution of Burst		Time Distribution of Burst			
E_0(eV)	E_0(eV)	E_0/E_0	Δt(μsec)	$\Delta t/t_0$	Δt_0(μsec)	$\Delta t_0/t_0$
0.005	0.0015	0.30			1008	0.195
					128 [b]	0.025 [b]

Resolution (inelastic):

Scattering Angles:

Range (degrees)	Number of Detector Banks	Flight Path (m)	Solid Angle per Detector Bank (steradian)	Kind of Detector
Fixed 90	3	5.03	0.0002	BF_3 190 cm pressure 2 in. diameter 20 in. long

[a] Chopper after sample, so that chopper transmission and duty cycle not included.

[b] Resolution as measured by the slope of the Be cutoff.

TABLE VI

COLD NEUTRON CHOPPER -- STUDSVIK

Instrument: Cold Neutron Chopper

Location: R2 Reactor Studsvik

Reference: Dahlborg, Larsson, and Sköld, Proceedings of the Bombay Conference on "Inelastic Scattering of Neutrons in Solids and Liquids", I.A.E.A. (1964).

Beam Size: 5 cm x 8 cm

Flight Path: 4.5 meters

Source Flux: 6×10^{13} thermal neutrons/cm^2-sec

Intensity Determination: Measured

Intensity:

E_0(eV)	I(n/min)	I(n/cm^2-min)
0.005	4.8×10^6 (With Chopper)	1.3×10^5 (With Chopper)

Resolution (elastic):

	Energy Distribution of Burst		Time Distribution of Burst		Burst Width at Detector	
E_0(eV)	ΔE_0(eV)	$\Delta E_0/E_0$	$\Delta\tau$(μsec)	$\Delta\tau/t_0$	Δt_0(μsec)	$\Delta t_0/t_0$
0.005	0.0007	0.15			53[a]	0.012[a]

Resolution (inelastic):

		Burst Width at Detector			Uncertainty in Energy Change	
E_0(eV)	E_f(eV)	Δt_f(μsec)	$\Delta t_f/t_f$	ε(eV)	$\Delta\varepsilon$(eV)	$\Delta\varepsilon/\varepsilon$
0.005	0.025	45	0.0225	0.020	0.0009	0.045

Signal/Background:

E_0(eV)	V Sample Thickness (cm)	Scattering Angle (degrees)	Signal/Background
0.005	1	90	30

Scattering Angles:

Range (degrees)	Number of Detector Banks	Flight Path (m)	Solid Angle per Detector Bank (steradians)	Kind of Detector
0 to 130	2	4.5	8.0×10^{-3}	3 cm x 30 cm 150 cm BF_3

[a] Resolution as measured by the slope of the Be cutoff.

TABLE VII

COLD NE[illegible] CHOPPER -- STOCKHOLM

Instrument: Cold Neutron Chopper No. 1

Location: R1 Reactor, Stockholm

Reference: Dahlborg, Larsson, and Sköld, Proceedings of the Bombay Conference on "Inelastic Scattering of Neutrons in Solids and Liquids", I.A.E.A. (1964).

Beam Size: 5 cm x 10 cm

Flight Path: 3.0 meters

Source Flux: 6×10^{11} thermal neutrons/cm^2-sec

Intensity Determination: Measured

Intensity:

E_0(eV)	I(n/min)	I(n/cm^2-min)
0.005	6.0×10^9 [a]	1.1×10^8 [a]

Resolution (elastic):

E_0(eV)	Energy Distribution of Burst		Time Distribution of Burst		Burst Width at Detector	
	ΔE_0(eV)	$\Delta E_0/E_0$	$\Delta\tau$(μsec)	$\Delta\tau/t_0$	Δt_0(μsec)	$\Delta t_0/t_0$
0.005	0.0025	0.5			60 [b]	0.02 [b]

Resolution (inelastic):

E_0(eV)	E_f(eV)	Burst Width at Detector		ε(eV)	Uncertainty in Energy Change	
		Δt_f(μsec)	$\Delta t_f/t_f$		$\Delta\varepsilon$(eV)	$\Delta\varepsilon/\varepsilon$
0.005	0.025	80	0.057	0.021	0.0027	0.13

Signal/Background:

E_0(eV)	V Sample Thickness (cm)	Scattering Angle (degrees)	Signal/Background
0.005	0.7	30	20

Scattering Angles:

Range (degrees)	Number of Detector Banks	Flight Path (m)	Solid Angle per Detector Bank (steradians)	Kind of Detector
0 to 90	1	3	6.0×10^{-3}	BF_3 1140 mm Hg 15 mm diameter (3 layers)

[a] Chopper after sample so those numbers do not include duty cycle or transmission of chopper. Duty cycle $\approx 3.0 \times 10^{-3}$.

[b] Resolution as measured by the slope of the Be cutoff.

TABLE VIII

COLD NEUTRON CHOPPER -- STOCKHOLM

Instrument: Cold Neutron Chopper No. 2

Location: R1 Reactor, Stockholm

Reference: Dahlborg, Larsson, and Sköld, Proceedings of the Bombay Conference on "Inelastic Scattering of Neutrons in Solids and Liquids", I.A.E.A. (1964).

Beam Size: 5 cm x 10 cm

Flight Path: 3.5 meters

Source Flux: 3×10^{11} thermal neutrons/cm^2-sec

Intensity Determination: Measured

Intensity:

E_o(eV)	I(n/min)	I(n/cm^2-min)
0.005	4.0×10^6	8.0×10^4

Resolution (elastic):

	Energy Distribution of Burst		Time Distribution of Burst		Burst Width at Detector	
E_o(eV)	ΔE_o(eV)	$\Delta E_o/E_o$	$\Delta\tau$(μsec)	$\Delta\tau/t_o$	Δt_o(μsec)	$\Delta t_o/t_o$
0.005	0.0015	0.3	96	0.028	490[a]	0.14[a]

Resolution (inelastic):

		Burst Width at Detector			Uncertainty in Energy Change	
E_o(eV)	E_f(eV)	Δt_f(μsec)	$\Delta t_f/t_f$	ε(eV)	$\Delta\varepsilon$(eV)	$\Delta\varepsilon/\varepsilon$
0.005	0.025					

Signal/Background:

E_o(eV)	V Sample Thickness (cm)	Scattering Angle (degrees)	Signal/Background
0.005	0.5	60	7

Scattering Angles:

Range (degrees)	Number of Detector Banks	Flight Path (m)	Solid Angle per Detector Bank (steradians)	Kind of Detector
0 to 115	4	3.5	6.0×10^{-3}	BF_3 1500 mm Hg 30 mm diameter

[a] Resolution as measured by the slope of the Be cutoff.

TABLE IX

COLD NEUTRON CHOPPER -- ISPRA

Instrument: Cold Neutron Chopper

Location: Ispra-I Reactor, EURATOM C.C.R. Ispra, Italy

Reference: Haas, Kley, Krebs, and Rubin (private communication).

Beam Size: 5 cm x 10 cm

Flight Path: 2.9 m/4.5 m

Source Flux: 0.8×10^{13} thermal neutrons/cm^2-sec

Intensity Determination: Measured

Intensity:

E_0(eV)	I(n/min)	I(n/cm^2-min)
0.005 (11,000 rpm[a])	3.5×10^7	7×10^5

Resolution (elastic):

	Energy Distribution of Burst		Time Distribution of Burst		Burst Width at Detector	
E_0(eV)	ΔE_0(eV)	$\Delta E_0/E_0$	$\Delta\tau$(μsec)	$\Delta\tau/t_0$	Δt_0(μsec)	$\Delta t_0/t_0$
0.005 (11,000 rpm[a])	0.00154	0.31	60	0.02	624	0.21

Resolution (inelastic)[b]:

		Burst Width at Detector			Uncertainty in Energy Change	
E_0(eV)	E_f(eV)	Δt_f(μsec)	$\Delta t_f/t_f$	ε(eV)	$\Delta\varepsilon$(eV)	$\Delta\varepsilon/\varepsilon$
0.005	0.025	230[c]	0.17	0.020	0.0088[d]	0.44

Signal/Background (2.9 m flight path -- no data for the 4.5 m flight path):

E_0(eV)	V Sample Thickness (cm)	Scattering Angle (degrees)	Signal/Background
0.005	0.28	90	11

Scattering Angles:

Range (degrees)	Number of Detector Banks	Flight Path (m)	Solid Angle per Detector Bank (steradian)	Kind of Detector
90	1	2.9	0.0143	BF_3
30 to 90	2	4.5	0.00593	BF_3

TABLE IX (Cont.)

COLD NEUTRON CHOPPER -- ISPRA

Comments: The data given for ΔE_0, $\Delta\tau$ and Δt_0 refer to the following system:

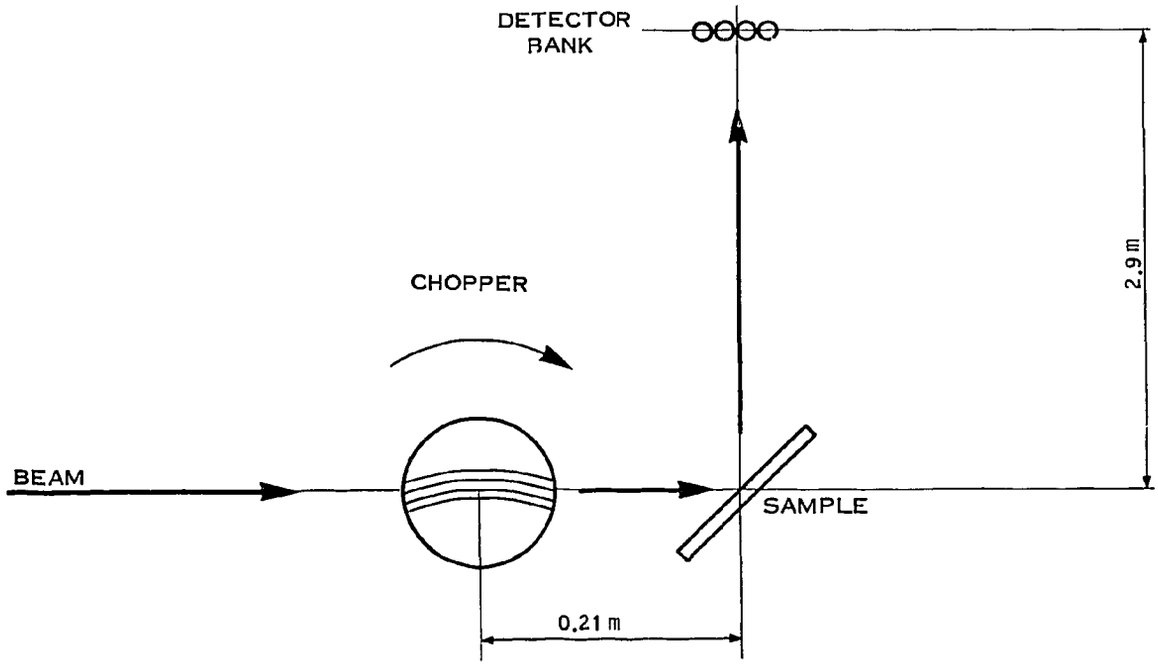

It is assumed that the calculated resolutions approximately represent this system.

[a] Angular velocity of chopper.

[b] Resolution for the 2.9 m flight path.

[c] Computed using Equation (2), with x = 1.04 given by Equation (1).

[d] Computed using Equation (3).

TABLE X

PHASED CHOPPER VELOCITY SELECTOR -- ISPRA

Instrument: Two Rotor Velocity Selector

Location: Ispra-I Reactor, EURATOM C.C.R. Ispra, Italy

Reference: K. H. Krebs (private communication).

Beam Size: 1.2 cm x 2 cm

Flight Path: 1.5 m

Source Flux: 2×10^{13} thermal neutrons/cm^2-sec

Intensity Determination: Calculated

Intensity:

E_o(eV)	I(n/min)	I(n/cm^2-min)
0.005 (13,300 rpm)	3.6×10^5	1.5×10^5
0.0136 (22,000 rpm)	1.8×10^6	7.5×10^5

Resolution (elastic)[a]:

	Energy Distribution of Burst		Time Distribution of Burst		Burst Width at Detector	
E_o(eV)	ΔE_o(eV)	$\Delta E_o/E_o$	$\Delta\tau$(μsec)	$\Delta\tau/t_o$	Δt_o(μsec)	$\Delta t_o/t_o$
0.005 (13,300 rpm)	0.00036	0.071	58	0.04	120	0.078
0.0136 (22,000 rpm)	0.00097	0.071	35	0.04	73	0.079

Resolution (inelastic)[a]:

		Burst Width at Detector			Uncertainty in Energy Change	
E_o(eV)	E_f(eV)	Δt_f(μsec)	$\Delta t_f/t_f$	ε(eV)	$\Delta\varepsilon$(eV)	$\Delta\varepsilon/\varepsilon$
0.005	0.025	74[b]	0.11	0.020	0.0055[c]	0.27
0.0136	0.025	55[b]	0.080	0.0114	0.0047[c]	0.41

Signal/Background:

Scattering Angles:

Range (degrees)	Number of Detector Banks	Flight Path (m)	Solid Angle per Detector Bank (steradian)	Kind of Detector
0 to 90	4	1 to 2	0.003 to 0.06	BF_3 Counters 70 cm pressure 5 cm OD x 40 cm effective length Li^6I Crystals 7.5 cm diameter

TABLE X (Cont.)

PHASED CHOPPER VELOCITY SELECTOR -- ISPRA

Comments: The data given for ΔE_0, $\Delta\tau$, and Δt_0 refer to the following systems:

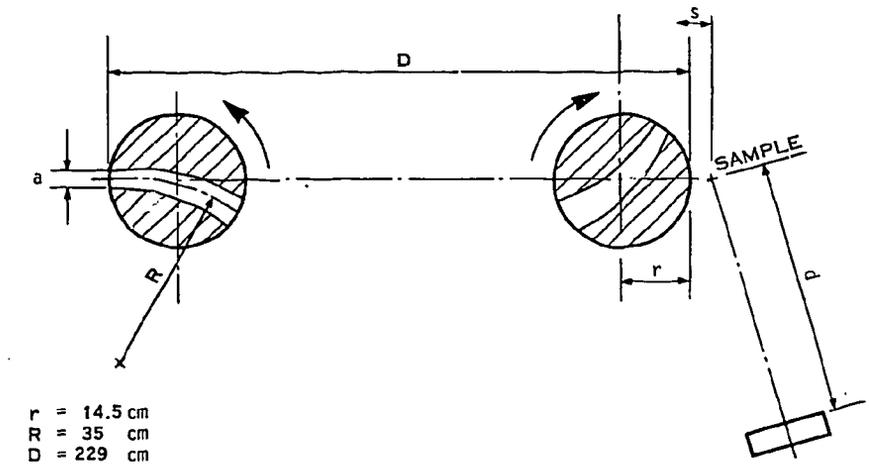

r = 14.5 cm
R = 35 cm
D = 229 cm
d = 150 cm
a = 1.2 cm

The following equations were used:

$$\Delta\tau = \frac{a}{\omega r}$$

$$\frac{\Delta E_0}{E_0} = 2\sqrt{2}\,\frac{\Delta\tau\, v_0}{D}\,.$$

[a] Assumed x = 1.15 + 0.5 = 1.65 where s = 0.5 (see comments above).

[b] Computed using Equation (2).

[c] Computed using Equation (3).

TABLE XI

ROTATING CRYSTAL SPECTROMETER -- ISPRA

Instrument: Rotating Crystal Spectrometer

Location: Ispra-I Reactor, EURATOM C.C.R. Ispra, Italy

Reference: Meister, Haas, and Kley (private communication).

Beam Size: 8 cm x 4.5 cm

Flight Path: 3.07 m

Source Flux: 2×10^{13} thermal neutrons/cm^2-sec

Intensity Determination: The intensities are deduced from the peak fluxes measured by gold activation in the stationary reflected neutron beam (higher order neutrons subtracted).

Intensity[a]:

E_0(eV)	I(n/min)	I(n/cm^2-sec)
0.005	2.5×10^4	7.0×10^2
0.025	2.5×10^5	7.0×10^3
0.060	4.5×10^5	1.2×10^4
0.125	1.5×10^5	4.0×10^3

Resolution (elastic)[a,b]:

	Energy Distribution of Burst		Time Distribution of Burst		Burst Width at Detector	
E_0(eV)	ΔE_0(eV)	$\Delta E_0/E_0$	$\Delta\tau$(μsec)	$\Delta\tau/t_0$	Δt_0(μsec)	$\Delta t_0/t_0$
0.005	0.00010	0.020	36	0.012	50	0.016
0.025	0.0004	0.016	35	0.023	36	0.026
0.060	0.0013	0.021	26	0.028	34	0.038
0.125	0.0035	0.028	20	0.032	28	0.045

Resolution (inelastic):

		Burst Width at Detector			Uncertainty in Energy Change	
E_0(eV)	E_f(eV)	Δt_f(μsec)	$\Delta t_f/t_f$	ε(eV)	$\Delta\varepsilon$(eV)	$\Delta\varepsilon/\varepsilon$
0.005	0.025	29[c]	0.021	0.020	0.0011[d]	0.055
0.060	0.025	57[c]	0.041	0.035	0.0050[d]	0.14
0.125	0.025	100[c]	0.072	0.100	0.012[d]	0.12

Signal/Background:

Scattering Angles:

Range (degrees)	Number of Detector Banks	Flight Path (m)	Solid Angle per Detector Bank (steradian)	Kind of Detector
0 to 110	1	3.07	0.012	BF_3 700 mm Hg pressure 5 cm diameter x 40 cm active length

TABLE XI (Cont.)

ROTATING CRYSTAL SPECTROMETER -- ISPRA

Comments: The data given refer to the following (preliminary) experimental layout:

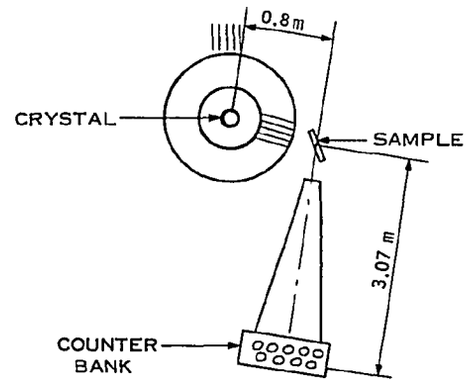

[a] For crystal 1-1/2 in. Ø turning with 6000 rpm.

[b] Scattering angle $\theta = 0$.

[c] Computed using Equation (2), with x = 1.0, 6.1, and 5.4 given by Equation (1).

[d] Computed using Equation (3).

TABLE XII

ROTATING CRYSTAL SPECTROMETER -- CHALK RIVER

Instrument: Rotating Crystal Spectrometer

Location: NRU Reactor, Chalk River

Reference: B. N. Brockhouse in Inelastic Scattering of Neutrons in Solids and Liquids, p 113, I.A.E.A., Vienna (1961), also A. D. B. Woods (private communication).

Beam Size: 2.5 cm x 5 cm

Flight Path: 3.3 m

Source Flux: 2×10^{14} thermal neutrons/cm^2-sec

Intensity Determination: Measured

Intensity:

E_0(eV)	I(n/min)	I(n/cm^2-min)
0.005	2.5×10^5	2×10^4
0.013	7.5×10^5	6×10^4
0.032	5×10^5	4×10^4
0.044	2.5×10^5	2×10^4

Resolution (elastic):

	Energy Distribution of Burst		Time Distribution of Burst		Burst Width at Detector	
E_0(eV)	ΔE_0(eV)	$\Delta E_0/E_0$	$\Delta\tau$(μsec)	$\Delta\tau/t_0$	Δt_0(μsec)	$\Delta t_0/t_0$
0.005		≈ 0.01[a]	28	0.0083	56	0.017
0.013		≈ 0.01[a]	20	0.010	36	0.017
0.032		≈ 0.01[a]	18	0.013	24	0.018
0.044		≈ 0.01[a]	16	0.014	22	0.020

Resolution (inelastic):

		Burst Width at Detector			Burst Width at Detector	
E_0(eV)	E_f(eV)	Δt_f(μsec)	$\Delta t_f/t_f$	ε(eV)	$\Delta\varepsilon$(eV)	$\Delta\varepsilon/\varepsilon$
0.005	0.025	43[b]	0.028	0.020	0.0014[c]	0.01
0.013	0.025	28[b]	0.019	0.012	0.0010[c]	0.083
0.032	0.025	22[b]	0.015	0.007	0.0010[c]	0.14
0.044	0.025	29[b]	0.019	0.019	0.0020[c]	0.10

[a] Calculated.

[b] Calculated from Equation (2) with x = 7.4, 6.3, 6.8, and 7.9 computed from Equation (1).

[c] Calculated from Equation (3).

TABLE XIII

ROTATING CRYSTAL SPECTROMETER -- KARLSRUHE

Instrument: Rotating Crystal Spectrometer

Location: FR2 Reactor, Kerforschungszentrum Karlsruhe

Reference: W. Glaser, I.A.E.A. Study Group Meeting on Research Reactor Experimental Techniques, October 1964, Bucharest; KFK-Report 263.

I. Beam Size: 3 cm x 7 cm
Flight Path: 2 meters

II. Beam Size: 4 cm x 5 cm
Flight Path: 3.5 meters

Source Flux: 8×10^{12} thermal neutrons/cm^2-sec[a]

Intensity Determination: Measured

Intensity:

	E_o(eV)	$2\theta_{BRAGG}$[b] (degrees)	I(n/min)	I(n/cm^2-min)
I.	0.085	24	3.4×10^5	1.6×10^4
	0.040	36	4.8×10^5	2.3×10^4
	0.020	52	3.4×10^5	1.6×10^4
II.	0.008	86	5.0×10^4	1.2×10^3

Resolution (elastic):

		Energy Distribution of Burst		Time Distribution of Burst		Burst Width at Detector	
	E_o(eV)	ΔE_o(eV)	$\Delta E_o/E_o$	$\Delta\tau$(μsec)	$\Delta\tau/t_o$	Δt_o(μsec)	$\Delta t_o/t_o$
I.[c]	0.085	0.0078	0.092	20	0.04	40	0.083
	0.040	0.0024	0.060	20	0.03	40	0.057
	0.020	0.0008	0.040	20	0.02	40	0.037
II.[d]	0.008	0.00008	0.01	20	0.007	40	0.015

Resolution (inelastic):

			Burst Width at Detector			Uncertainty in Energy Changes	
	E_o(eV)	E_f(eV)	Δt_f(μsec)	$\Delta t_f/t_f$	ε(eV)	$\Delta\varepsilon$(eV)	$\Delta\varepsilon/\varepsilon$
I.	0.085	0.025	40[e]	0.10	0.060	0.03[e]	≈ 0.05
	0.040	0.025	40[e]	0.10	0.015	0.03[e]	≈ 0.2
	0.020	0.025	40[e]	0.10	0.005	0.03[e]	≈ 0.6
II.	0.008	0.025	40[e]	0.10	0.017	0.03[e]	≈ 0.2

Signal/Background:

E_o(eV)	V Sample Thickness (cm)	Scattering Angle (degrees)	Signal/Background
0.085	0.2	135	10
0.040	0.2	135	20
0.040	0.2	145	33
0.020	0.2	145	9
0.020	0.2	135	10

TABLE XIII (Cont.)

ROTATING CRYSTAL SPECTROMETER -- KARLSRUHE

Scattering Angles:

Range (degrees)	Number of Detector Banks	Flight Path (m)	Solid Angle per Detector Bank (steradian)	Kind of Detector
20 to 150	9	2	0.003	He^3 & Li^6-ZnS

[a] To be increased X7 late 1965.

[b] Al crystal (111).

[c] One collimator before the crystal (15 minutes of angle): crystal at 14,000 rpm.

[d] Second collimator behind the crystal.

[e] Extracted from experimental values.

TABLE XIV

PHASED ROTOR NEUTRON SPECTROMETER -- CHALK RIVER

Instrument: Phased Rotor Neutron Spectrometer (to be dismantled 1966).

Location: A.E.C.L. Chalk River

Reference: D. I. Page (private communication).

Beam Size: 2.5 cm x 5.0 cm

Flight Path: 1.7 m for 1st Quadrant Detectors
1.3 m for 3rd Quadrant Detectors
3.0 m for 4th Quadrant Detectors (narrow angle array)

Source Flux: 1.2×10^{14} thermal neutrons/cm^2-sec

Intensity Determination: Measured

Intensity:

E_o(eV)	I(n/min)	I(n/cm^2-sec)
0.10	6.3×10^5	4.9×10^4
0.055	7.2×10^5	5.6×10^4
0.025	2.6×10^5	2.0×10^4

Resolution (elastic)[a]:

	Energy Distribution of Burst		Time Distribution of Burst		Burst Width at Detector	
E_o(eV)	ΔE_o(eV)	$\Delta E_o/E_o$	$\Delta\tau$(μsec)	$\Delta\tau/t_o$	Δt_o(μsec)	$\Delta t_o/t_o$
0.10[b]	0.00195	0.195	6	0.009[c]	12.26[c]	0.018[c]
0.055[b]	0.00076	0.0138	6	0.0065[c]	11.65[c]	0.0125[c]
0.025[b]	0.00026	0.0104	6	0.0044[c]	12.35[c]	0.009[c]
0.10[b]	0.00195	0.0195	6	0.016[d]	10.0[d]	0.026[d]
0.055[b]	0.00076	0.0138	6	0.012[d]	8.96[d]	0.017[d]
0.025[b]	0.00026	0.104	6	0.0078[d]	9.32[d]	0.12[d]
0.10[b]	0.00195	0.0195	6	0.021[e]	9.3[e]	0.0315[e]
0.055[b]	0.00076	0.0138	6	0.015[e]	8.68[e]	0.0215[e]
0.025[b]	0.00026	0.0104	6	0.010[e]	9.5[e]	0.016[e]

Resolution (inelastic)[a]:

		Burst Width at Detector			Uncertainty in Energy Change	
E_o(eV)	E_f(eV)	Δt_f(μsec)	$\Delta t_f/t_f$	ε(eV)	$\Delta\varepsilon$(eV)	$\Delta\varepsilon/\varepsilon$
0.10[b]	0.025	57.8[c]	0.042[c]	0.075	0.00415[c]	0.055[c]
0.055[b]	0.025	19.3[c]	0.0207[c]	0.030	0.0027[c]	0.09[c]
0.10[b]	0.025	34.9[d]	0.045[d]	0.075	0.00568[d]	0.075[d]
0.055[b]	0.025	13.1[d]	0.0249[d]	0.030	0.0035[d]	0.117[d]
0.10[b]	0.025	27.8[e]	0.047[e]	0.075	0.0068[e]	0.089[e]
0.055[b]	0.025	11.3[e]	0.0279[e]	0.030	0.00453[e]	0.151[e]

Signal/Background:

E_o(eV)	V Sample Thickness (cm)	Scattering Angle (degrees)	Signal/Background
0.1	0.36	10 to 90	≈ 50
0.1	0.36	90 to 160	≈ 25
0.017	0.36	4 to 22	≈ 10

TABLE XIV (Cont.)

PHASED ROTOR NEUTRON SPECTROMETER -- CHALK RIVER

Scattering Angles:

Range (degrees)	Number of Detector Banks	Flight Path (m)	Solid Angle per Detector Bank (steradian)	Kind of Detector
10 to 90	15	1.7	0.00383	LiF·ZnS Scintillation
90 to 160	9	1.3	0.00872	
4 to 22	10	3.0	0.00129	

[a] Assuming x = 1.85.

[b] Rotors at 30,000 rpm.

[c] 3 m flight path.

[d] 1.7 m flight path.

[e] 1.3 m flight path.

TABLE XV

PHASED CHOPPER VELOCITY SELECTOR (EQUAL SLOT CHOPPERS) -- MATERIALS TESTING REACTOR

Instrument: Phased Chopper Velocity Selector[a]

Location: Materials Testing Reactor, NRTS, Idaho Falls, Idaho

Reference: Gavin, Harker, and Brugger (private communication).

Beam Size: 3.38 cm x 10.16 cm

Flight Path: 2 meters

Source Flux: 2×10^{14} thermal neutrons/cm^2-sec

Intensity Determination: Measured

Intensity:

E_0(eV)	I(n/min)	I(n/cm^2-min)
0.10[b]	2.9×10^6	8.5×10^4
0.076[c]	1.2×10^6	3.5×10^4
0.055[c]	2.4×10^6	7.0×10^4
0.042[c]	1.7×10^6	5.0×10^4

Resolution (elastic):

	Energy Distribution of Burst		Time Distribution of Burst		Burst Width at Detector	
E_0(eV)	ΔE_0(eV)	$\Delta E_0/E_0$	$\Delta\tau$(μsec)	$\Delta\tau/t_0$	Δt_0(μsec)	$\Delta t_0/t_0$
0.10[b]	0.0027[d]	0.026	6.5	0.014	14.7[e]	0.032
0.076[c]	0.0018[d]	0.024	6.5	0.012	14.7[e]	0.028
0.055[c]	0.0011[d]	0.020	6.5	0.010	14.7[e]	0.024
0.042[c]	0.0007[d]	0.017	6.5	0.009	14.7[e]	0.021

Resolution (inelastic):

		Burst Width at Detector			Uncertainty in Energy Change	
E_0(eV)	E_f(eV)	Δt_f(sec)	$\Delta t_f/t_f$	ε(eV)	$\Delta\varepsilon$(eV)	$\Delta\varepsilon/\varepsilon$
0.10	0.025	56[f]	0.061	0.075	0.0071[g]	0.095
0.076	0.025	40[f]	0.044	0.051	0.0048[g]	0.094
0.055	0.025	28[f]	0.031	0.030	0.0031[g]	0.10
0.042	0.025	21[f]	0.023	0.017	0.0021[g]	0.12

Signal/Background:

Scattering Angles:

Range (degrees)	Number of Detector Banks	Flight Path (m)	Solid Angle per Detector Bank	Kind of Detector
15 to 145	15	2 to 2.25	0.007 to 0.029	BF_3 167 cm pressure 1 in. ID, 18 in. long
2.8 to 20	15	2.5	0.0004 to 0.0008	BF_3 167 cm pressure 1 in. ID, 4 in. long
2.0 to 10	15	2.25	0.0006 to 0.0012	He^3 10 Atm 1 in. ID, 6 in. long

[a] Both choppers have equal speeds and slot widths.

[b] 83 in. radius of curvature curved slits in rotors. Choppers at 12,000 rpm.

TABLE XV (Cont.)

PHASED CHOPPER VELOCITY SELECTOR
(EQUAL SLOT CHOPPERS) -- MATERIALS TESTING REACTOR

[c] 42 in. radius of curvature curved slits in rotors. Choppers at 12,000 rpm.

[d] Computed from Equation (1) using Δt_0 values at two distances from the chopper (2 beam monitors).

[e] Measured.

[f] Computed from Equation (2) with x = 2.6 computed from Equation (1).

[g] Computed from Equation (3).

TABLE XVI

PHASED CHOPPER VELOCITY SELECTOR (UNEQUAL SLOT CHOPPERS) -- MATERIALS TESTING REACTOR

Instrument: Phased Chopper Velocity Selector[a]

Location: Materials Testing Reactor, NRTS, Idaho Falls, Idaho

Reference: R. M. Brugger (private communication).

Beam Size: 3.38 cm x 10.16 cm

Flight Path: 2.25 meters

Source Flux: 2×10^{14} thermal neutrons/cm^2-sec

Intensity Determination: Measured

Intensity:

E_0(eV)	I(n/min)	I(n/cm^2-min)
0.07[b]	2.9×10^6	1.0×10^5
0.05[b]	3.1×10^6	1.1×10^5
0.03[b]	1.4×10^6	4.8×10^4

Resolution (elastic)[c]:

	Energy Distribution of Burst		Time Distribution of Burst		Burst Width at Detector	
E_0(eV)	E_0(eV)	$\Delta E_0/E_0$	$\Delta\tau$(μsec)	$\Delta\tau/t_0$	Δt_0(μsec)	$\Delta t_0/t_0$
0.07	0.0020	0.038	6.5	0.010	19.4	0.031
0.05	0.0012	0.032	6.5	0.009	19.4	0.027
0.03	0.0006	0.025	6.5	0.007	19.4	0.020

Resolution (inelastic)[c]:

		Burst Width at Detector			Uncertainty in Energy Change	
E_0(eV)	E_f(eV)	Δt_f(μsec)	$\Delta t_f/t_f$	ε(eV)	$\Delta\varepsilon$(eV)	$\Delta\varepsilon/\varepsilon$
0.07	0.025	62	0.0602	0.045	0.0053	0.12
0.05	0.025	35	0.034	0.025	0.0032	0.13
0.03	0.025	24	0.023	0.005	0.0017	0.34

[a] Both choppers have equal speeds. Slot width of first chopper is 2x that of second chopper.

[b] 42 in. radius of curvature curved slits in rotors. Choppers at 12,000 rpm.

[c] Assumed x = 1.34.

TABLE XVII

ROTATING CRYSTAL SPECTROMETER -- BATTELLE-NORTHWEST LABORATORY

Instrument: Rotating Crystal Spectrometer with Phased Chopper
Location: Battelle-Northwest Laboratory, Richland, Washington
Reference: O. K. Harling (private communication).
Beam Size: 2.5 x 10.16 cm[a]
Flight Path: 1.5 m[b]
Source Flux:
Intensity Determination: Measured and Calculated
Intensity:

	E_0(eV)	I(n/min)	I(n/cm^2-min)
I.	0.300[c]	12.0 x 10^5	4.64 x 10^4
II.	0.300[c]	3.0 x 10^5	1.16 x 10^4
III.	0.300[c]	0.75 x 10^5	0.29 x 10^4

Resolution (elastic):

		Energy Distribution of Burst		Time Distribution of Burst[d]		Burst Width at Detector[e]	
	E_0(eV)	ΔE_0(eV)	$\Delta E_0/E_0$	$\Delta\tau$(μsec)	$\Delta\tau/t_0$	Δt_0(μsec)	$\Delta t_0/t_0$
I.	0.3[c]	0.0132	0.044	7.0	0.035	13.3	0.066
II.	0.3[c]	0.0066	0.022	6.0	0.031	7.3	0.037
III.	0.3[c]	0.0029	0.0097	4.7	0.024	4.9	0.025
IV.	0.1[c]	0.0009	0.009	6.5	0.019	7.5	0.022
V.	0.5[c]	0.013	0.026	5.0	0.033	5.5	0.036

Resolution (inelastic):

			Burst Width at Detector			Uncertainty in Energy Change[f]	
	E_0(eV)	E_f(eV)	Δt_f(μsec)	$\Delta t_f/t_f$	ε(eV)	$\Delta\varepsilon$(eV)	$\Delta\varepsilon/\varepsilon$
I.	0.3[c]	0.025	180	0.26	0.275	0.0186	0.068
II.	0.3[c]	0.025	93	0.14	0.275	0.0093	0.034
III.	0.3[c]	0.025	43	0.060	0.275	0.0041	0.015
IV.	0.1[c]	0.025	21	0.03	0.075	0.001	0.013
V.	0.5[c]	0.025	190	0.28	0.475	0.015	0.032

Signal/Background:

E_0(eV)	V Sample Thickness (cm)	Scattering Angle (degrees)	Signal/Background
0.017	0.225	90	17.5

TABLE XVII (Cont.)

ROTATING CRYSTAL SPECTROMETER -- BATTELLE-NORTHWEST LABORATORY

Scattering Angles:

Range (degrees)	Number of Detector Banks	Flight Path (m)	Solid Angle per Detector Bank (steradian)	Kind of Detector
15 to 165	11	1.0 and 1.5	0.0065 to 0.033	BF_3 1 in. ID, 10 in. long, 2 Atm
		1.0 and 1.5	0.0043 to 0.030	He^3 1 in. ID, 15 in. long, 8 Atm

[a] Can be increased to 5 cm in width.

[b] Can be decreased to 1.0 meter.

[c] With Cu[220] planes in transmission mode. Crystal rotating at 12,000 rpm
I. Collimator 0.36° II., IV., V. Collimator 0.18° III. Collimator 0.079°

[d] Burst measured at sample.

[e] Δt_0 given is for a 15° scattering angle.

[f] $\Delta\varepsilon$ was calculated from $\Delta\varepsilon^2 = \left(\frac{2\Delta t_f}{t_f}\right)^2 + \Delta E_0^{\,2}$, where ΔE_0 is the Bragg energy uncertainty in the incident beam. This method of calculating $\Delta\varepsilon$ differs from that used in Equation 3 of this compilation. For the Battelle Rotating Crystal Spectrometer the contribution of the energy spread is small compared to the total time spread in the incident neutron pulse, ie, $\frac{\Delta E_0}{E_0} < \frac{2\Delta t_0}{t_0}$ under normal operating conditions. Therefore use of Equation 3 would overestimate the error in $\Delta\varepsilon$.

TABLE XVIII

LINAC NEUTRON VELOCITY SELECTOR -- GENERAL ATOMICS

Instrument: General Atomic Neutron Velocity Selector (10,800 rpm) (in operation)

Location: General Atomic Electron LINAC

Reference: W. L. Whittemore (private communication).

Beam Size: 7.0 cm x 25.4 cm

Flight Path: 2.0 meters

Source Flux: Not Determined Directly

Intensity Determination: Measured

Intensity:

E_o(eV)	I(n/min)	I(n/cm^2-min)
0.167[a]	6.7 x 10^5[b]	3.8 x 10^3[b]
0.233[a]	5.5 x 10^5[b]	3.1 x 10^3[b]
0.41[a]	5.5 x 10^5[b]	3.1 x 10^3[b]

Resolution (elastic):

	Energy Distribution of Burst		Time Distribution of Burst		Burst Width at Detector	
E_o(eV)	ΔE_o(eV)	$\Delta E_o/E_o$	$\Delta\tau$(μsec)	$\Delta\tau/t_o$	Δt_o(μsec)	$\Delta t_o/t_o$
0.167[a]	0.0062	0.370	19	0.0539	26	0.0743
0.233[a]	0.0101	0.0436	19	0.0634	26	0.0861
0.410[a]	0.0238	0.0580	19	0.0841	26	0.1150

Resolution (inelastic):

		Burst Width at Detector			Uncertainty in Energy Change	
E_o(eV)	E_f(eV)	Δt_f(μsec)	$\Delta t_f/t_f$	ε(eV)	$\Delta\varepsilon$(eV)	$\Delta\varepsilon/\varepsilon$
0.167	0.025	125[c]	0.148	0.142	0.0259[d]	0.182
0.233	0.025	198[c]	0.218	0.208	0.0417[d]	0.200
0.410	0.025	450[c]	0.495	0.385	0.0971[d]	0.251

Signal/Background:

E_o(eV)	V Sample Thickness (cm)	Scattering Angle (degrees)	Signal/Background
0.167	0.19	60	3.6 (8.0)[e]
0.233	0.19	60	5.4 (9.5)[e]
0.410	0.19	60	3.5 (6.6)[e]

TABLE XVIII (Cont.)

LINAC NEUTRON VELOCITY SELECTOR -- GENERAL ATOMICS

Scattering Angles:

Range (degrees)	Number of Detector Banks	Flight Path (m)	Solid Angle per Detector Bank (steradian)	Kind of Detector
30 ± 1.75[f]	1	2.0[g]	0.0032 to 0.016	He^3 1 in. ID, 20 in. long, 10 Atm
60 ± 3.5[f]	1	2.0[g]	0.0032 to 0.032	BF_3 1 in. ID, 20 in. long, 167 cm
90 ± 3.5[f]	1	2.0[g]	0.0064 to 0.032	BF_3 2 in. ID, 20 in. long, 90 cm
120 ± 3.5[f]	1	2.0[g]	0.0064 to 0.032	BF_3 2 in. ID, 20 in. long, 90 cm
150 ± 3.5[f]	1	2.0[g]	0.0064 to 0.032	BF_3 2 in. ID, 20 in. long, 90 cm

[a] 120 in. radius of curvature.

[b] Output for LINAC with 400 mA and 28 MeV electrons, Tungsten target, and a 1.5-in. H_2O moderator; uranium target gives an increase by a factor of 2; improvements in GA LINAC expected by January 1966 will increase neutron output by another factor of 2.

[c] Computed from Equation (2), with x = 4.8 computed from Equation (1).

[d] Computed from Equation (3).

[e] Parentheses indicate signal at peak to background.

[f] The angular range can be reduced if circumstances require this improved angular resolution.

[g] This flight path can be increased to ≈ 3.0 m, if necessary.

TABLE XIX

LINAC NEUTRON VELOCITY SELECTOR -- GENERAL ATOMICS

Instrument: General Atomic Neutron Velocity Selector (14,400 rpm) (expected)

Location: General Atomic Electron LINAC

Reference: W. L. Whittemore (private communication).

Beam Size: 7.0 cm x 25.4 cm

Flight Path: 2.0 meters

Source Flux: Not Determined Directly

Intensity Determination: Measured

Intensity:

E_0(eV)	I(n/min)	I(n/cm^2-min)
0.167[a]	6.7 x 10^5[b]	3.8 x 10^3[b]
0.233[a]	5.5 x 10^5[b]	3.1 x 10^3[b]
0.41[a]	5.5 x 10^5[b]	3.1 x 10^3[b]

Resolution (elastic):

	Energy Distribution of Burst		Time Distribution of Burst		Burst Width at Detector	
E_0(eV)	ΔE_0(eV)	$\Delta E_0/E_0$	$\Delta\tau$(μsec)	$\Delta\tau/t_0$	Δt_0(μsec)	$\Delta t_0/t_0$
0.167[a]	0.00456	0.0273	14	0.0395	19	0.0539
0.233[a]	0.00749	0.0321	14	0.0467	19	0.0631
0.410[a]	0.01741	0.0426	14	0.0630	19	0.0840

Resolution (inelastic):

		Burst Width at Detector			Uncertainty in Energy Change	
E_0(eV)	E_f(eV)	Δt_f(μsec)	$\Delta t_f/t_f$	ε(eV)	$\Delta\varepsilon$(eV)	$\Delta\varepsilon/\varepsilon$
0.167	0.025	93[c]	0.101	0.142	0.0187[d]	0.132
0.233	0.025	146[c]	0.161	0.208	0.0306[d]	0.148
0.410	0.025	328[c]	0.360	0.385	0.0700[d]	0.182

[a] 120 in. radius of curvature.

[b] Output for LINAC with 400 mA and 28 MeV electrons, Tungsten target, and a 1.5-in. H_2O moderator; uranium target gives an increase by a factor of 2; improvements in GA LINAC expected by January 1966 will increase neutron output by another factor of 2.

[c] Computed from Equation (2), with x = 4.5 computed from Equation (1).

[d] Computed from Equation (3).

TABLE XX

LINAC NEUTRON VELOCITY SELECTOR -- RENSSELAER POLYTECHNIC INSTITUTE

Instrument: Phased Linac-Chopper Velocity Selector (old 14,400 rpm chopper)

Location: Linear Accelerator Laboratory, Rensselaer Polytechnic Institute, Troy, New York

Reference: Seemann, Moore, and Kirouac (private communication).

Beam Size: 2.54 cm x 3.80 cm

Flight Path: 1.87 m

Source Flux: 1.1×10^{11} neutrons/sec eV into 4π steradians at 25 KW average electron beam power

Intensity Determination: Measured

Intensity:

E_o(eV)	I(n/min)	I(n/cm^2-min)
0.20	0.7×10^5	5.4×10^3
0.50	1.2×10^5	9.3×10^3
1.00	2.5×10^5	1.9×10^4

Resolution (elastic):

	Energy Distribution of Burst		Time Distribution of Burst		Burst Width at Detector	
E_o(eV)	ΔE_o(eV)	$\Delta E_o/E_o$	$\Delta\tau$(μsec)	$\Delta\tau/t_o$	Δt_o(μsec)	$\Delta t_o/t_o$
0.20	0.011	0.055	15.5	0.051	28	0.093
0.50	0.040	0.080	15.5	0.082	28	0.15
1.00	0.115	0.115	15.5	0.11	27	0.20

Resolution (inelastic):

		Burst Width at Detector			Uncertainty in Energy Change	
E_o(eV)	E_f(eV)	Δt_f(μsec)	$\Delta t_f/t_f$	ε(eV)	$\Delta\varepsilon$(eV)	$\Delta\varepsilon/\varepsilon$
0.20	0.025	200[a]	0.23	0.175	0.038[b]	0.22
0.50	0.025	700[a]	0.82	0.475	0.14[b]	0.30
1.00	0.025	1985[a]	2.32	0.975	0.42[b]	0.43

[a] Computed from Equation (2), with x = 4.0, 4.5, and 4.1 computed from Equation (1).

[b] Computed from Equation (3).

TABLE XXI

PHASED CHOPPER VELOCITY SELECTOR -- RENSSELAER POLYTECHNIC INSTITUTE

Instrument: Phased Linac-Chopper Velocity Selector[a] (new 30,000 rpm chopper)

Location: Linear Accelerator Laboratory, Rensselaer Polytechnic Institute, Troy, New York

Reference: Seeman, Moore, and Kirouac (private communication).

Beam Size: 5.08 cm x 10.16 cm

Flight Path: 2.37 m

Source Flux: 1.1×10^{11} neutrons/sec eV at 0.5 eV into 4π steradians at 25 kW average electron beam power

Intensity Determination: Calculated from source flux

Intensity:

E_o(eV)	I(n/min)	I(n/cm^2-min)
0.20[b]	4.3×10^5	8.3×10^3
0.50[c]	3.6×10^5	7.0×10^3
1.00[d]	2.9×10^6	5.7×10^4

Resolution (elastic):

	Energy Distribution of Burst		Time Distribution of Burst		Burst Width at Detector	
E_o(eV)	ΔE_o(eV)	$\Delta E_o/E_o$	$\Delta\tau$(μsec)	$\Delta\tau/t_o$	Δt_o(sec)	$\Delta t_o/t_o$
0.20[b]	0.006	0.030	15.7	0.041	23	0.060
0.50[c]	0.015	0.030	11.8	0.048	14	0.058
1.00[d]	0.042	0.042	7.8	0.043	12	0.067

Resolution (inelastic):

		Burst Width at Detector			Uncertainty in Energy Change	
E_o(eV)	E_f(eV)	Δt_f(μsec)	$\Delta t_f/t_f$	ε(eV)	$\Delta\varepsilon$(eV)	$\Delta\varepsilon/\varepsilon$
0.20[b]	0.025	140[e]	0.13	0.175	0.024[f]	0.14
0.50[c]	0.025	330[e]	0.31	0.475	0.069[f]	0.13
1.00[d]	0.025	920[e]	0.85	0.975	0.14[f]	0.14

[a] Operation scheduled for August 1965.

[b] 85 in. radius of curvature for chopper slits, chopper at 15,000 rpm.

[c] 85 in. radius of curvature for chopper slits, chopper at 20,000 rpm.

[d] 85 in. radius of curvature for chopper slits, chopper at 30,000 rpm.

[e] Computed from Equation (2), with x = 6.0, 5.0, and 4.6 computed from Equation (1).

[f] Computed from Equation (3).

TABLE XXII

COLD NEUTRON CHOPPER -- BUCHAREST

Instrument: Cold Neutron Chopper

Location: VVR-S Reactor, Bucharest

Reference: Teutsch, Mateescu, Nahorniak, Diaconescu and Timis, Revue Roumaine de Physique 9, p 737 (1964)[a].

Beam Size: 4 cm x 4 cm

Flight Path: 2.4 m

Source Flux: 2×10^{12} thermal neutrons/cm^2-sec

Intensity Determination: Calculated

Intensity:

E_0(eV)	I(n/min)	I(n/cm^2-min)
0.005	4.5×10^5[b]	3.0×10^4[b]

Resolution (elastic):

E_0(eV)	Energy Distribution of Burst		Time Distribution of Burst		Burst Width at Detector	
	ΔE_0(eV)	$\Delta E_0/E_0$	$\Delta\tau$(μsec)	$\Delta\tau/t_0$	Δt_0(μsec)	$\Delta t_0/t_0$
0.005	0.0014	0.28	90[c]	0.033[c]	445	0.17
					90[d]	0.033[d]

Resolution (inelastic):

E_0(eV)	E_f(eV)	Burst Width at Detector		ε(eV)	Uncertainty in Energy Change	
		Δt_f(μsec)	$\Delta t_f/t_f$		$\Delta\varepsilon$(eV)	$\Delta\varepsilon/\varepsilon$
0.005	0.025	118	0.11	0.020	0.0055	0.28

Signal/Background:

E_0(eV)	V Sample Thickness (cm)	Scattering Angle (degrees)	Signal/Background
0.005	0.35	90	30

Scattering Angles:

Range (degree)	Number of Detector Banks	Flight Path (m)	Solid Angle per Detector Bank (steradian)	Kind of Detector
15 to 90	1	2.4	0.024	10 B-10F_3 300 mm Hg 4 cm diameter 35 cm long

[a] A new Be filter, 34 cm long, is used and the chopper was placed in front of the sample.

[b] To be increased by cooling the filter.

[c] Total error including sweep-time, channel width, etc.

[d] Error for the Be cutoff ($\Delta E_0 = 0$), characteristic for elastic and guasi-elastic measurements with the filter-method.

TABLE XXIII

NEUTRON CHOPPER -- MOL

Instrument: Cold and Thermal Neutron Chopper

Location: BR2, Mol (Belgium), Beam Tube R2

Reference: W. Van Dingenen (private communication). Paper in preparation (Nuclear Instruments and Methods).

Beam Size: 6 cm x 6 cm

Flight Path: 4.5 meters

Source Flux: 9×10^{13} thermal neutrons/cm^2-sec

Intensity Determination: Measured

Intensity:

	E_0(eV)	I(n/min)	I(n/cm^2-min)
Be-filtered cold neutron beam:	0.005 to 0.004	1.5×10^8	5.5×10^6
Monochromatic cold neutron beam:	0.005	1.3×10^7 (with chopper)	4.6×10^5 (with chopper)
Monochromatic thermal beams are provided:	No data yet		

Resolution (elastic) (at 5000 rpm):

	Energy Distribution of Burst		Time Distribution of Burst		Burst Width at Detector	
E_0(eV)	ΔE_0(eV)	$\Delta E_0/E_0$	$\Delta\tau$(μsec)	$\Delta\tau/t_0$	Δt_0(μsec)	$\Delta t_0/t_0$
0.005	0.00015	0.025	100		93	0.02

Resolution (inelastic) (at 5000 rpm):

		Burst Width at Detector			Uncertainty in Energy Change	
E_0(eV)	E_f(eV)	Δt_f(μsec)	$\Delta t_f/t_f$	ε(eV)	$\Delta\varepsilon$(eV)	$\Delta\varepsilon/\varepsilon$
0.005	0.025	71[a]	0.03	0.020	0.0015	0.075

Signal/Background:

E_0(eV)	V Sample Thickness (cm)	Scattering Angles (degrees)	Signal/Background
0.005	0.3	90	66

Scattering Angles:

Range (degrees)	Number of Detector Banks	Flight Path (m)	Solid Angle per Detector Bank (steradian)	Kind of Detector
0 to 120	1[b]	4.5	0.00033	2 layers of 2 in. enriched BF_3 detectors (20th Century), 18 in. long, 70 cm pressure

[a] Computed from Equation (2) with x = 0.28 calculated from Equation (1).

[b] Eight banks are under project.

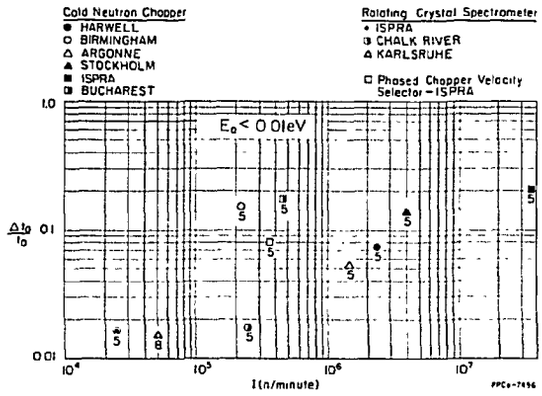

Fig. 1 The full width at half maximum of a burst of elastically scattered neutrons as measured at the detector divided by their mean time of flight from the sample to the detector, $\Delta t_0/t_0$, versus the beam intensity, I(n/min) for incident energies less than 10 meV. The number next to each symbol denotes the incident energy in meV associated with that point.

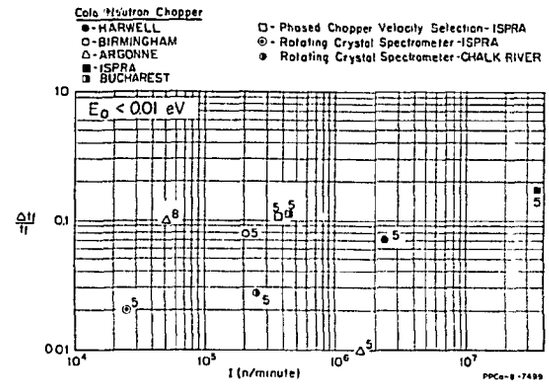

Fig. 2 The full width at half maximum of a burst of inelastically scattered neutrons as measured at the detector divided by their mean time of flight from the sample to the detector, $\Delta t_f/t_f$, versus the beam intensity, I(n/min), for incident energies less than 10 meV. The number next to each symbol denotes the incident energy in meV associated with that point. For this compilation, the mean energy of the inelastically scattered neutrons was chosen to be 25 meV.

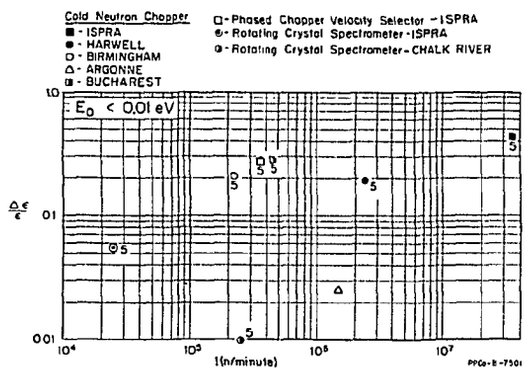

Fig. 3 The uncertainty in measuring the energy change divided by the energy change, $\Delta\varepsilon/\varepsilon$, versus the beam intensity, I(n/min), for incident energies less than 10 meV. The number next to each symbol denotes the incident energy in meV associated with that point. For this compilation, the mean energy of the inelastically scattered neutrons was chosen to be 25 meV.

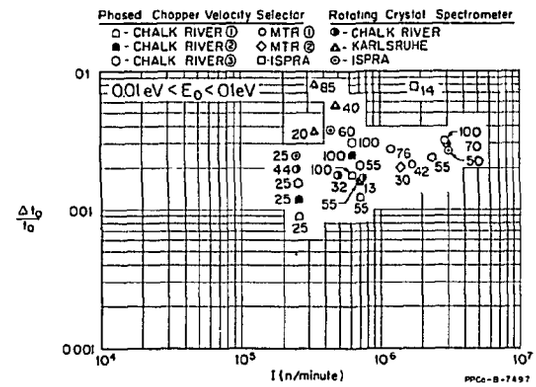

Fig. 4 The full width at half maximum of a burst of elastically scattered neutrons as measured at the detector divided by their mean time of flight from the sample to the detector, $\Delta t_0/t_0$, versus the beam intensity, I(n/min), for incident energies between 10 and 100 meV. The number next to each symbol denotes the incident energy in meV associated with that point.

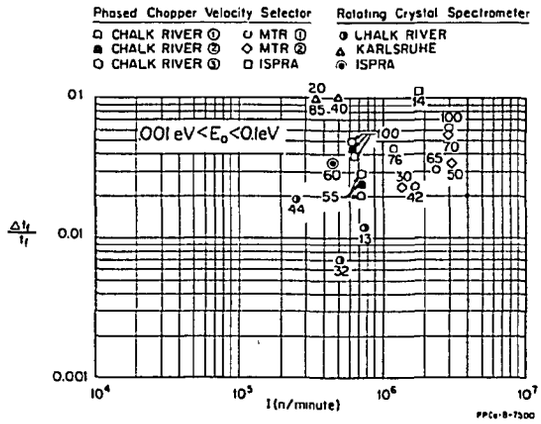

Fig. 5 The full width at half maximum of a burst of inelastically scattered neutrons as measured at the detector divided by their mean time of flight from the sample to the detector, $\Delta t_f/t_f$, versus the beam intensity, I(n/min), for incident energies between 10 and 100 meV. The number next to each symbol denotes the incident energy in meV associated with that point. For this compilation, the final mean energy of the inelastically scattered neutrons was chosen to be 25 meV.

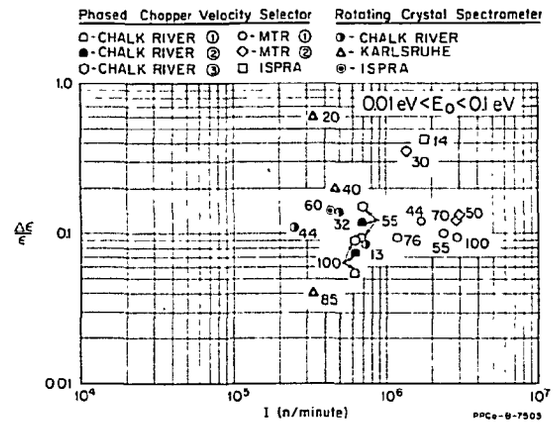

Fig. 6 The uncertainty in measuring the energy change divided by the energy change, $\Delta\epsilon/\epsilon$, versus the beam intensity, I(n/min), for incident energies between 10 and 100 meV. The number next to each symbol denotes the incident energy in meV associated with that point. For this compilation, the mean energy of the inelastically scattered neutrons was chosen to be 25 meV.

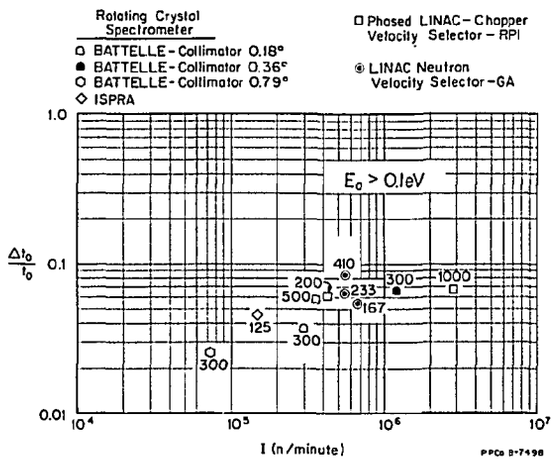

Fig. 7 The full width at half maximum of a burst of elastically scattered neutrons as measured at the detector divided by their mean time of flight from the sample to the detector, $\Delta t_o/t_o$, versus the beam intensity, I(n/min), for incident energies greater than 100 meV. The number next to each symbol denotes the incident energy in meV associated with that point.

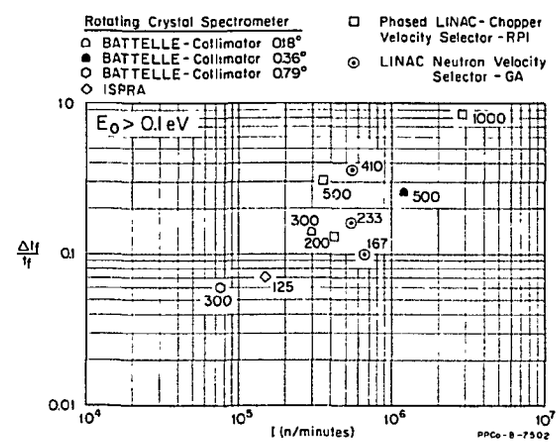

Fig. 8 The full width at half maximum of a burst of inelastically scattered neutrons as measured at the detector divided by their mean time of flight from the sample to the detector, $\Delta t_f/t_f$, versus the beam intensity, I(n/min), for incident energies greater than 100 meV. The number next to each symbol denotes the incident energy in meV associated with that point. For this compilation, the mean energy of the inelastically scattered neutrons was chosen to be 25 meV.

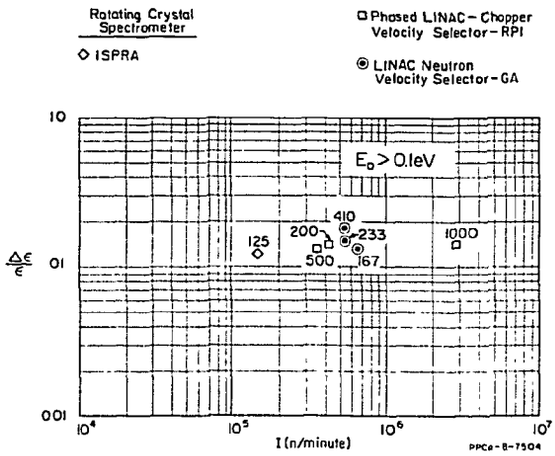

Fig. 9 The uncertainty in measuring the energy change divided by the energy change, $\Delta\varepsilon/\varepsilon$, versus the beam intensity, I(n/min), for incident energies greater than 100 meV. The number next to each symbol denotes the incident energy in meV associated with that point. For this compilation, the mean energy of the inelastically scattered neutrons was chosen to be 25 meV.

PHILLIPS
PETROLEUM
COMPANY

PHILLIPS 66

ATOMIC ENERGY DIVISION